Dynamical immunization strategy for seasonal epidemics

Shu Yan,[1,*] Shaoting Tang,[1,†] Sen Pei,[1] Shijin Jiang,[2] and Zhiming Zheng[1,‡]
[1]*LMIB and School of Mathematics and Systems Science, Beihang University, Beijing 100191, China*
[2]*School of Mathematical Sciences, Peking University, Beijing 100871, China*
(Received 30 May 2014; published 19 August 2014)

The topic of finding an effective strategy to halt virus in a complex network is of current interest. We propose an immunization strategy for seasonal epidemics that occur periodically. Based on the local information of the infection status from the previous epidemic season, the selection of vaccinated nodes is optimized gradually. The evolution of vaccinated nodes during iterations demonstrates that the immunization tends to locate in both global hubs and local hubs. We analyze the epidemic prevalence using a heterogeneous mean-field method, and we present numerical simulations of our model. This immunization performs better than some other previously known strategies. Our work highlights an alternative direction in immunization for seasonal epidemics.

DOI: 10.1103/PhysRevE.90.022808 PACS number(s): 89.75.Hc, 87.23.Ge

I. INTRODUCTION

Epidemic spreading in complex networks has received considerable attention for the past two decades [1–8]. The immunization strategy to halt virus is an important topic in epidemic spreading research, and most of the previous literature in this field has focused on the selection of vaccinated nodes before the outbreak of an epidemic [9–19]. Numerous immunization strategies have been proposed, such as uniform immunization (nodes are vaccinated randomly) [9,14] or targeted immunization (most highly connected nodes are vaccinated) [10,14]. Targeted immunization is a highly effective vaccination strategy [8], but it requires global information about the network, thus making it impractical in real cases. Cohen *et al*. proposed acquaintance immunization strategy [11], based on the immunization of a small fraction of random neighbors of randomly selected nodes. Its principle can be described as a higher-degree node that is easier to choose from a random link. Without specific knowledge of the network, this method is efficient for networks of any broad-degree distribution, and it allows for a relatively low threshold of immunization. In addition, some other novel immunization strategies have been proposed in the past decade [16–19], and they have applications in different cases.

However, many infectious diseases outbreak seasonally, which is not fully discussed in the previous literature as far as we know [20,21]. The periodic change of temperature, humidity profiles, or even the succession of school terms and holidays can lead to periodic phenomena of epidemics. Previous data have shown that outbreaks in rubella, whooping cough, and influenza reveal obvious seasonality [22]. A simple explanation of epidemics presenting seasonal phenomena is as follows: After spreading extensively, a virus dies out because infected individuals have recovered and produced antibodies. But in the next epidemic season, the mutated virus propagates again, rendering a new outbreak of the epidemic. This process then occurs repeatedly.

Herein, we propose an immunization strategy for seasonal epidemics to give a better description of this phenomenon. We merely adopt uniform immunization on the network at first. Before the start of the next epidemic season, we adjust the vaccinated nodes according to the infection status of their neighbors in the previous epidemic season. This process does not require global information of the network, and it achieves better performance than uniform immunization and acquaintance immunization under the same circumstances.

In this paper, we adopt the susceptible-infected-recovered (SIR) model [22–24] as the epidemic spreading model, and we analyze the epidemic prevalence using a heterogeneous mean-field method [25]. We introduce some parameters to investigate the evolution of vaccinated nodes during iterations, which is the main focus of the paper, and we find that some nodes in the network will be selected multiple times, although not always continuously. As epidemic season continues, the selection of vaccinated individuals tends to be stable. Those nodes include both global hubs, who possess most connections, and local hubs, who are influential in their communities. In addition, we also present some numerical results of our strategy on certain real social networks. The proposed strategy can be applied efficiently in real cases, and it highlights a new direction in immunization of seasonal epidemics.

The strategy will be introduced in detail in Sec. II. The analytical results and numerical simulations are presented in Secs. III and IV, respectively. Finally, conclusions are drawn in Sec. V, and relevant prospects are discussed.

II. DYNAMICAL IMMUNIZATION STRATEGY

We consider a connected and undirected network with N nodes. In every epidemic season, there are two stages: the vaccinating process and the epidemic spreading process. During the vaccinating process, we select some nodes using a certain strategy and we vaccinate them. Vaccinated nodes cannot be infected nor can they spread epidemic to others. After vaccinating, the epidemic begins to spread, following the dynamics of the SIR model. Each unvaccinated node in the network can be in one of the three states (susceptible, infected, or recovered). Susceptible nodes are still healthy. They catch the disease via direct contact with infected nodes at a rate β. Infected nodes will recover and become recovered nodes with

*yanshu@smss.buaa.edu.cn
†tangshaoting@buaa.edu.cn
‡zzheng@pku.edu.cn

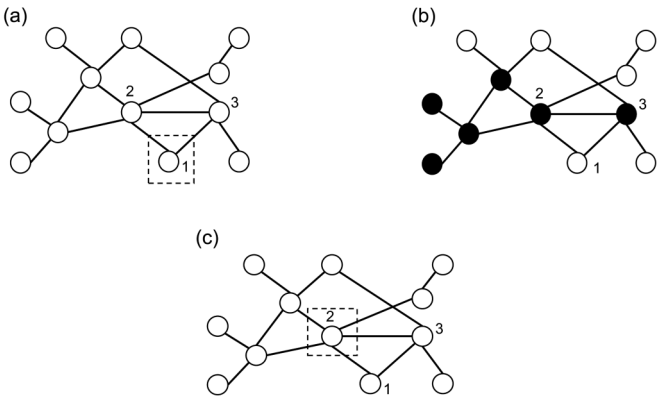

FIG. 1. An illustration of our dynamical immunization strategy. First in (a), we randomly assign node 1 as the vaccinated node. After the epidemic spreading process, the system state is shown in (b). White nodes stand for susceptible nodes while black nodes denote recovered nodes. We calculate the W value of node 1 and its neighbors, i.e., node 2 and node 3. Since $W(1) = 2$, $W(2) = 4$, and $W(3) = 2$, node 2 replaces node 1 as the new vaccinated node in the next epidemic season, as shown in (c).

a rate μ. Without loss of generality, we set $\mu = 1$ henceforth. Initially, we set an unvaccinated node as the epidemic seed, and other unvaccinated nodes are susceptible nodes. We focus on the proportion of recovered nodes, r_∞, when the epidemic process dies out in one epidemic season, i.e., when no infected nodes are left in the system.

We denote the vaccinated proportion by v. In the first epidemic season, vN vaccinated nodes are selected randomly. That is to say, we perform a uniform immunization strategy on the network initially. We define $W(u)$ as the number of infected nodes among the set $\Gamma(u) \cup \{u\}$, where $\Gamma(u)$ denotes the set of u's neighbors. In the second epidemic season, we adjust the vaccinated nodes according to the epidemic spreading result in the first season. For every vaccinated node u in epidemic season $S-1$, we calculate $W(u)$ and $W(v)$ for all $v \in \Gamma(u)$ in epidemic season S. Of all these nodes, we vaccinate the node who has the maximal value of W since the W value implies the epidemic status of the node. Thus, the new vaccinated node derived from node u is $\arg\max_{y\in\Gamma(u)\cup\{u\}} W(y)$. An illustration of our strategy is shown in Fig. 1.

Note that if two different vaccinated nodes (u and v) induce the same new vaccinated node w in the next epidemic season, we then select one node at random, say u, and set the new vaccinated node that u induces as $\arg\max_{y\in\Gamma(u)\cup\{u\}\setminus v} W(y)$. However, if the new node that node u induces is already immunized, we then seek the node who has the second largest W value (in u and u's neighbors), and this procedure can be repeated. Of all these cases, if no appropriate neighbor can be chosen, the vaccinated node remains unchanged.

After the selection of vaccinated nodes, the epidemic spreads again. The epidemic spreading process in this season is independent of the previous results, i.e., the epidemic seed is randomly selected from unvaccinated nodes, and other unvaccinated nodes are all susceptible. After the epidemic, we then select new vaccinated nodes according to the epidemic results. The vaccinating process and the epidemic spreading process occur in cycles.

In every vaccinating process, we calculate the W value for $\langle k\rangle vN$ nodes on average. Calculating the W value for every node requires its $\langle k\rangle$ neighbors' information. Therefore, the complexity of our algorithm is $O(N)$, meaning that this strategy can be applied to networks with large size.

What we need to point out is that the time scale for seasonal epidemics between outbreaks is of year order, and the network topology can be changed to a certain extent. Our model ignores this aspect and assumes the structure is static.

Obviously, we do not need the information from the entire network structure during the immunization process. Therefore, it is a local strategy.

III. THEORETICAL ANALYSIS

In this section, we establish a simple theoretical framework of our strategy. Here we adopt a heterogeneous mean-field method [25] in which nodes are characterized by their degrees. The first and second moments of the network are $\langle k\rangle = \sum kP(k)$ and $\langle k^2\rangle = \sum k^2P(k)$, where $P(k)$ is the degree distribution of the network. The proportion of susceptible, infected, and recovered nodes at time t is $s(t)$, $i(t)$, and $r(t)$, respectively. Due to the immunization property, the proportion of vaccinated nodes remains unchanged. Thus, we have $s(t) + i(t) + r(t) = 1 - v$. Let $v_k^{(S)}$ represent the probability that a node with degree k is chosen to be vaccinated at season S. Naturally, it holds that $\sum P(k)v_k^{(S)} = v$.

At season $S = 1$, we apply uniform immunization, i.e., $v_k^{(1)} \equiv v$. The introduction of a density v of immune individuals chosen at random is equivalent to a simple rescaling of the epidemic spreading rate as β to $\beta(1-v)$, i.e., the rate at which new infected nodes appear is decreased by a factor proportional to the probability that they are not immunized. We denote the density of susceptible, infected, and recovered nodes in the degree class k at epidemic season S by $s_k^{(S)}$, $i_k^{(S)}$, and $r_k^{(S)}$, respectively. The SIR model evolution reads [26]

$$\begin{aligned}\frac{di_k^{(1)}}{dt} &= \beta(1-v)ks_k^{(1)}\Theta^{(1)} - i_k^{(1)},\\ \frac{ds_k^{(1)}}{dt} &= -\beta(1-v)ks_k^{(1)}\Theta^{(1)},\\ \frac{dr_k^{(1)}}{dt} &= i_k^{(1)}.\end{aligned} \tag{1}$$

The initial conditions are $i_k^{(1)}(0) = i_0$, $r_k^{(1)}(0) = 0$, and $s_k^{(1)}(0) = 1 - i_0$ for any k. In the equation above, $\Theta^{(1)}$ stands for the average density of infected individuals at vertices pointed by any given edge at $S = 1$. Assuming the network structure is uncorrelated [27], we have

$$\Theta^{(1)} = \frac{\sum_k (k-1)P(k)i_k^{(1)}(t)}{\langle k\rangle}. \tag{2}$$

Using the method presented in Ref. [28], we can obtain that the total epidemic prevalence in season $S = 1$ is [26]

$$r^{(1)}(\infty) = \sum_k P(k)(1 - e^{-\beta(1-v)k\phi_\infty}), \tag{3}$$

where ϕ_∞ satisfies

$$\phi_\infty = 1 - \frac{1}{\langle k\rangle} - \frac{1}{\langle k\rangle}\sum_k (k-1)P(k)e^{-\beta(1-v)k\phi_\infty}. \quad (4)$$

Moreover, the immunization threshold (for uniform immunization) is [26]

$$v_c = 1 - \frac{\langle k\rangle}{\beta(\langle k^2\rangle - \langle k\rangle)}. \quad (5)$$

Using the numerical method, we can calculate $r_k^{(1)}$ by Eq. (1). Since we have assumed that the network is uncorrelated, the probability that an individual has a neighbor with degree k is $\eta(k) \equiv kP(k)/\sum kP(k)$. Therefore, the probability that a node with degree k has l recovered neighbors is $\binom{k}{l}(p^{(1)})^l[1-(p^{(1)})]^{(k-l)}$, where $p^{(1)} = \sum_{i=1}^{k_m}\eta(i)r_i^{(1)}$, and k_m is the maximal degree of the network. Due to the property of binomial distribution, the expectation of the number of recovered neighbors that a node with degree k has is $kp^{(1)}$, and the probability that the node itself is a recovered node is $r_k^{(1)}$. Thus we have $W_k^{(1)} = kp^{(1)} + r_k^{(1)}$, where $W_k^{(S)}$ is the W value of the node with degree k in season S. For convenience, we assume that the probability that a node is chosen to be the new vaccinated node is proportional to its W value. Therefore, we derive that the probability that a node with degree k is immunized in the epidemic season $S = 2$ is

$$v_k^{(2)} = \frac{\left(kp^{(1)} + r_k^{(1)}\right)v}{\sum\left(kp^{(1)} + r_k^{(1)}\right)P(k)}. \quad (6)$$

Then, the dynamical equation of epidemic spreading in season $S = 2$ is

$$\begin{aligned}\frac{di_k^{(2)}}{dt} &= \beta\left(1 - v_k^{(2)}\right)ks_k^{(2)}\Theta^{(2)} - i_k^{(2)},\\ \frac{ds_k^{(2)}}{dt} &= -\beta\left(1 - v_k^{(2)}\right)ks_k^{(2)}\Theta^{(2)},\\ \frac{dr_k^{(2)}}{dt} &= i_k^{(2)}.\end{aligned} \quad (7)$$

Similarly, we can obtain $r_k^{(2)}$ for $k = 1,2,\ldots,k_m$ and $r_\infty^{(2)} = \sum_k P(k)r_k^{(2)}$. The iterative process can be applied recursively, and a series of $r_\infty^{(S)}$ ($S = 2,3,\ldots$) can be obtained by Eq. (8):

$$\begin{aligned}\frac{di_k^{(S)}}{dt} &= \beta\left(1 - v_k^{(S)}\right)ks_k^{(S)}\Theta^{(S)} - i_k^{(S)},\\ \frac{ds_k^{(S)}}{dt} &= -\beta\left(1 - v_k^{(S)}\right)ks_k^{(S)}\Theta^{(S)},\\ \frac{dr_k^{(S)}}{dt} &= i_k^{(S)},\end{aligned} \quad (8)$$

where $v_k^{(S)}$ satisfies

$$v_k^{(S)} = \frac{\left(kp^{(S-1)} + r_k^{(S-1)}\right)v}{\sum\left(kp^{(S-1)} + r_k^{(S-1)}\right)P(k)}, \quad (9)$$

and $p^{(S-1)} = \sum_{i=1}^{k_m}\eta(i)r_i^{(S-1)}$.

We adopt some Barabási-Albert (BA) networks [29] to verify our results. The BA network is a classic heterogeneous network topology, and it has highly skewed degree distribution. Because it is not a trivial process to solve Eq. (8) in extremely large networks, here we select networks with $N = 100$, 500, and 1000 [shown in Figs. 2(a), 2(b), and 2(c), respectively].

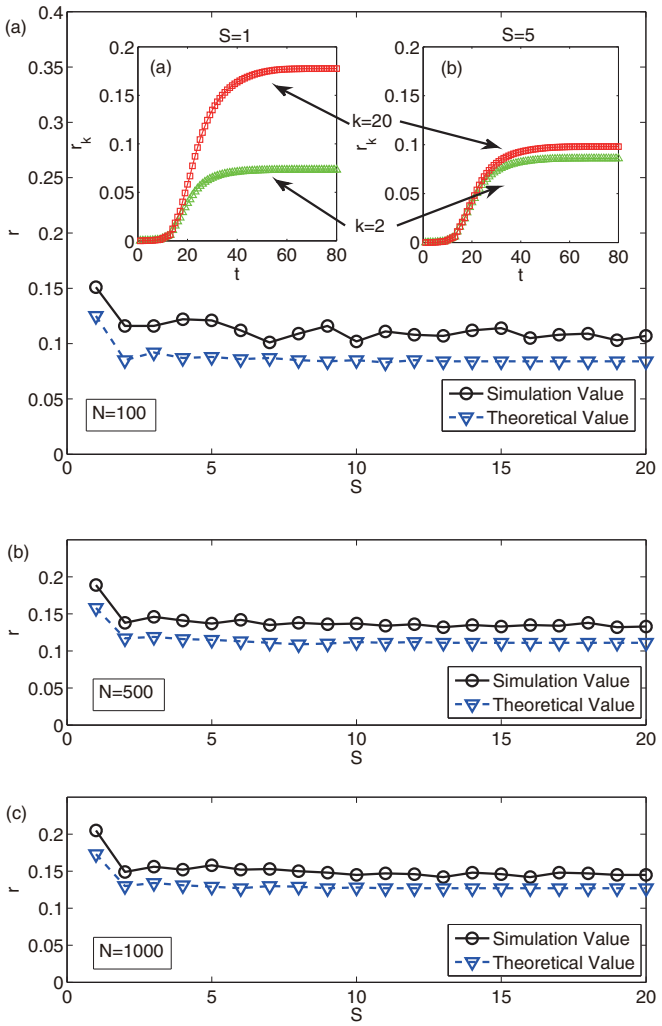

FIG. 2. (Color online) The comparison between simulation values and theoretical values for $r_\infty^{(S)}$. Results of the BA network with $N = 100$, 500, and 1000 are shown in (a), (b), and (c), respectively. The black circles denote the simulation value while the blue dashed line denotes the theoretical value. Inset of (a): The relationship of $r_k^{(S)}$ and time step t. The left figure is for $S = 1$ while the right figure is for $S = 5$. Top curves (red squares) stand for $k = 20$, and bottom curves (green triangles) stand for $k = 2$. Epidemic parameters are $\beta = 0.1$ and $v = 0.1$. Each simulation point is the average value of 10^2 experiments.

In the main plot of Fig. 2(a), we compare the simulation value with the theoretical value. The numerical results are relatively consistent with the simulation. The insets in Fig. 2(a) present the relationship between $r_k^{(S)}(t)$ and the time step t. The left figure is for $S = 1$, while the right figure is for $S = 5$. The top curves (red squares) stand for $k = 20$, and the bottom curves (green triangles) stand for $k = 2$. Compared with uniform immunization ($S = 1$), our method significantly decreases the epidemic prevalence for higher-degree nodes.

It can be observed that there is a discrepancy between the theoretical values and simulations. This discrepancy might be caused by analytical approximations (especially in the calculation of the W value). In addition, the mean-field method in which nodes with the same degree are regarded as the same, as well as the numerical solutions of the equations, may also inevitably introduce some errors.

IV. SIMULATION RESULTS

In this section, we further investigate our strategy using numerical simulations. To start with, we perform our strategy in a BA network with $N = 100$ to make it visually clear.

Figure 3 shows the evolution of vaccinated nodes. The dark red (solid) nodes denote vaccinated nodes while the light blue (hollow) nodes denote unvaccinated nodes. Figure 4 presents some statistical properties of the entire network and the vaccinated nodes from $S = 1$ to 6, including the averaged degree, the average k-shell number [30], and the average path length [28]. The degree and the k-shell number describe the importance of a node, and the average path length among nodes implies their closeness [8]. As illustrated in Fig. 4, for vaccinated nodes, the average degree and the average k-shell obtain their maximal values (average path length obtains its minimal value) at $S = 2$, but the epidemic prevalence obtains its minimal value at $S = 6$. It shows that, in this case, a higher average degree and a higher average k-shell number do not necessarily lead to a better immunizing effect. In addition, the selection of vaccinated nodes in our strategy is not a periodic process, but rather an optimizing process. Comparing Fig. 3(b) with Fig. 3(d), we may find that hubs are prone to be selected as vaccinated nodes in the second epidemic season. Nevertheless, it is not the best status because vaccinated nodes are too centralized, and numerous peripheral nodes are not covered. The situation is improved as the evolution continues. As can be seen from Fig. 3(f), in the sixth epidemic season, some "local hubs," which do not have the highest degree value but may connect some communities or peripheral nodes closely, are included. Thus, our method is not only concerned with connections or k-shell numbers of a node, but it also considers the nodes who have important locations in the network [31,32].

However, the simulation on a network with only 100 nodes is obviously inconclusive. We need to enlarge the network size and adopt networks with more realistic structures. Thus we adopt four real networks [33]: (i) Wikipedia Vote Network: Wikipedia is a free encyclopedia written collaboratively by volunteers around the world. Nodes in the network represent Wikipedia users, and a directed edge from node i to node j indicates that user i voted on user j. (ii) Epinions Social Network: This is a who-trusts-whom online social network

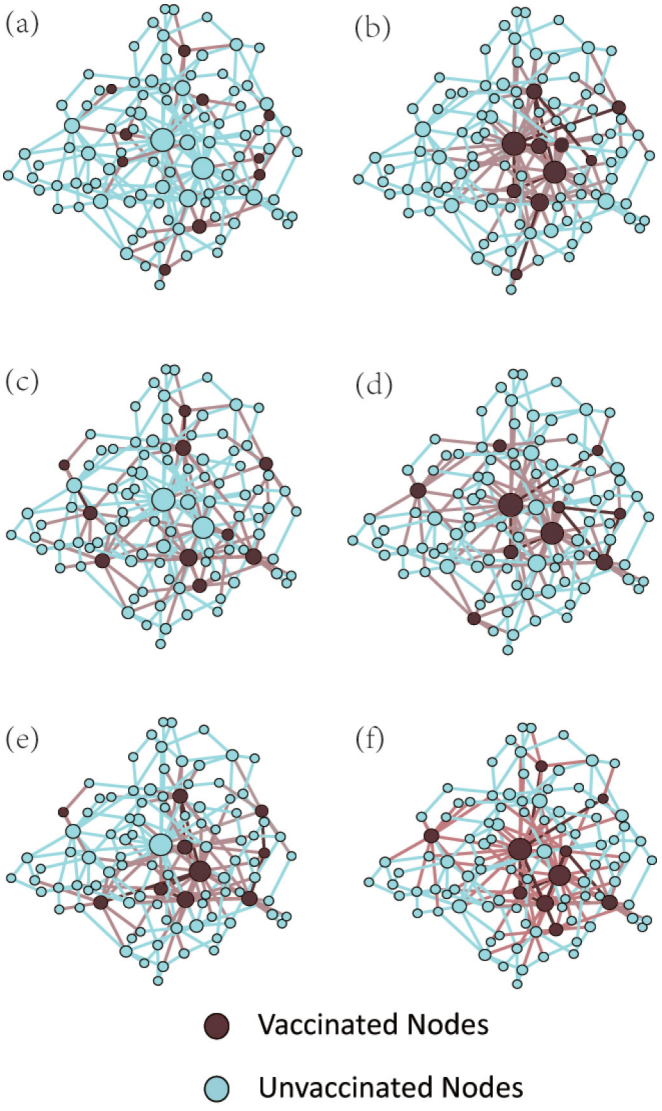

FIG. 3. (Color online) A demonstration of immunization for $S = 1$–6 [(a)–(f)]. Here we adopt a BA network with $N = 100$ and $\langle k \rangle = 3.94$. Epidemic parameters are $\beta = 0.1$ and $v = 0.1$. The size of the node implies its degree. Dark red (solid) nodes stand for vaccinated nodes, while light blue (hollow) nodes stand for unvaccinated nodes. We merely show the immunization situation, neglecting the epidemic spreading results.

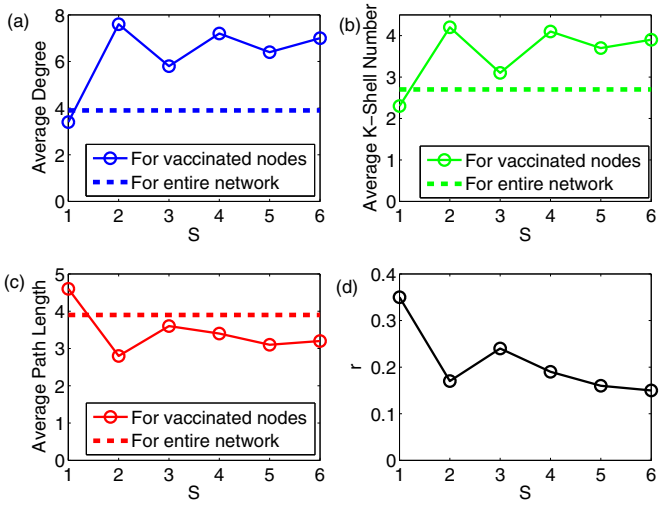

FIG. 4. (Color online) The curves of average degree (a), average k-shell (b), and average path length (c) in the BA network. The dashed lines represent the value of the entire network, and the circles represent the corresponding value among vaccinated nodes. The epidemic prevalence is shown in (d). Network structure is shown in Fig. 3. Epidemic parameters are $\beta = 0.1$ and $v = 0.1$.

TABLE I. The statistics of four real networks.

Name	N	$\langle C\rangle$	$\langle k\rangle$	$\langle k^2\rangle$	v_c ($\beta = 0.1$)	v_c ($\beta = 0.05$)
Wiki-Vote	7115	0.14	29.4	4554.8	0.935	0.870
Epinions	75879	0.14	16.4	3172.1	0.955	0.909
Slashdot	77360	0.06	23.5	6428.8	0.963	0.927
Enron	36692	0.50	22.5	6812.1	0.967	0.934

of a general consumer review site Epinions.com. Nodes in the network represent Epinions users and edges represent trust relationships. (iii) Slashdot Social Network: Slashdot is a technology-related news website known for its specific user community. The network contains links between the users of Slashdot. (iv) Enron Email Network: Enron email communication network covers email communication within an email dataset. Nodes of the network are email addresses, and if an address i sent at least one email to address j, the graph contains an edge from i to j.

Although these four networks are online social networks or email networks, they have spreading properties similar to actual interpersonal networks that are hard to obtain [34–36]. The statistics of these four networks are listed in Table I, where $\langle C\rangle$ stands for the average clustering coefficient of the network [4]. We treat all directed links as undirected links. It should be pointed out that we do not consider the directionality because the actual background of epidemic spreading is undirected. It is shown in the table that v_c is too large to be obtained, implying that the total immunity is hard to reach. This is a reflection of the finding that a heterogeneous network is an ideal substrate for epidemic spreading [2,37].

We now compare our method with other classic immunization strategies, such as uniform immunization, targeted immunization, and acquaintance immunization. Note that these immunization strategies are independent of the epidemic season. We average the results of 100 experiments and show the results for Wiki-Vote network, Epinions network, Slashdot network, Enron network, the above BA network with $N = 100$, and a BA network with $N = 100\,000$ in Figs. 5(a)–5(f), respectively. Generally, our method performs better than uniform immunization and acquaintance immunization after a few seasons, but it is inferior to targeted immunization. Comparing Figs. 5(e) and 5(f), we could conclude that the larger the network size is, the more efficient the targeted immunization is. Yet the fact that it requires global information makes it impractical in real cases. Thus, our strategy compromises between immunization efficiency and limited information. It should also be pointed out that as v increases, the difference between our algorithm and targeted immunization is becoming smaller. However, it is unrealistic that v is very large in real cases.

As is shown in Fig. 5, the epidemic prevalence of our method gradually decreases to a steady state, but not monotonically. The fluctuation can be interpreted as follows. In a particular epidemic season S, some influential spreaders (i.e., who play important roles in the spreading process) are vaccinated. Therefore, it is relatively difficult for their neighbors to be infected in the next epidemic season $S + 1$, and they are not chosen to be the vaccinated nodes due to the fact that they have fewer infected neighbors. While the new

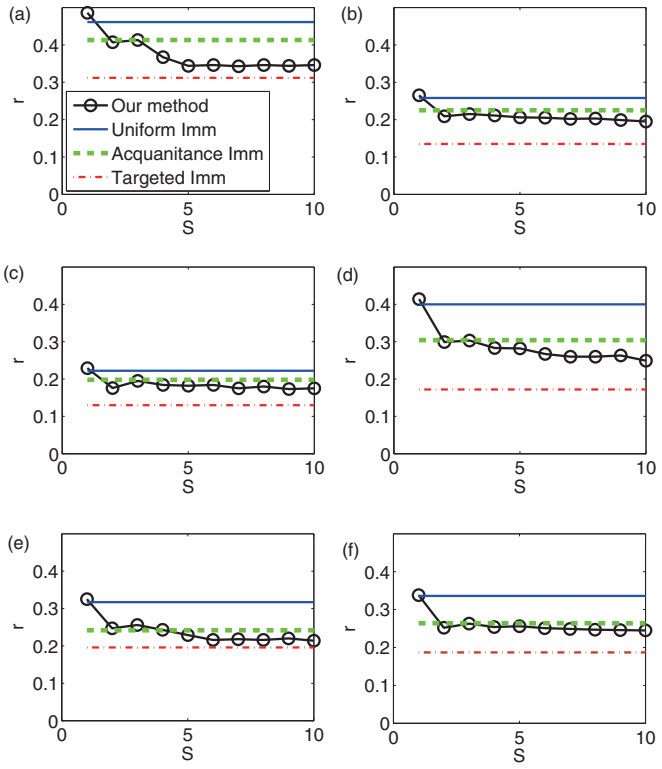

FIG. 5. (Color online) The relationship between epidemic prevalence $r_\infty^{(S)}$ and epidemic season S for different immunization strategies. Black circles stand for our dynamical immunization method. Three lines represent uniform immunization (blue, solid), acquaintance immunization (green, dashed), and targeted immunization (red, dash-dotted) from top to bottom. Results of Wiki-Vote network, Epinions network, Slashdot network, Enron network, BA network with $N = 100$, and BA network with $N = 10^6$ are shown in (a)–(f), respectively. Epidemic parameters are $\beta = 0.1$ and $v = 0.1$. Each point is the average value of 10^2 experiments.

vaccinated nodes are less influential than those nodes, the infected populations of epidemic season $S + 1$ increase. In the epidemic season $S + 2$, those influential nodes are set to be vaccinated nodes again, which lessens the risk of the epidemic.

Then we introduce recurrence rates $Q_1(S)$ and $Q_2(S)$ to investigate the overlapping of vaccinated nodes. Here $Q_1(S)$ is the proportion of nodes vaccinated in both epidemic seasons S and $S - 1$ ($S = 2,3,\ldots$), and $Q_2(S)$ is the proportion of nodes vaccinated in both epidemic seasons S and $S - 2$ ($S = 3,4,\ldots$). For example, if there are G common nodes that are vaccinated both in epidemic seasons S and $S - 1$, then $Q_1(S) = G/(vN)$. These parameters reflect the fluctuation of the evolution and are graphically presented in Fig. 6. As epidemic season continues, $Q_1(S)$ rises while $Q_2(S)$ shows a decreasing trend in general. But when S is large enough, $Q_2(S)$ is prone to increase and finally maintains a relatively steady level. This implies that some nodes have a higher probability of being vaccinated repeatedly.

Figure 6 shows the overlapping of vaccinated nodes in epidemic seasons S and $S - 1$ ($S - 2$), but it does not provide information about how many nodes are vaccinated continuously. To illustrate this issue clearly, we introduce $A_{S'}(S)$, which is defined as the proportion of nodes that have

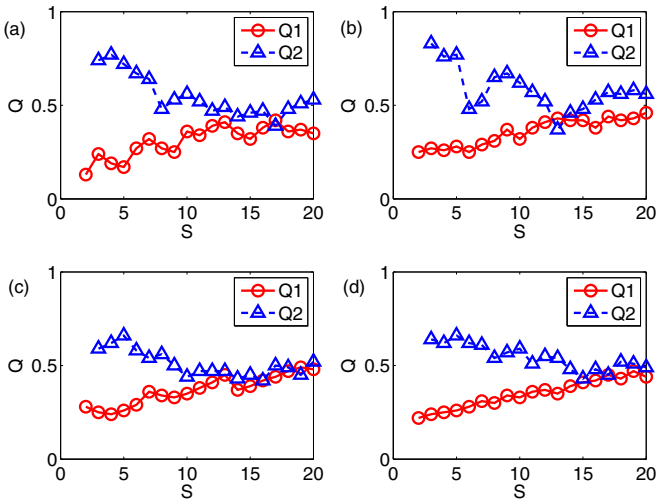

FIG. 6. (Color online) The relationship between recurrence rate $Q_1(S)$ [$Q_2(S)$] and epidemic season S. The red circles stand for $Q_1(S)$ and the blue triangles for $Q_2(S)$. Results of Wiki-Vote network, Epinions network, Slashdot network, and Enron network are shown in (a), (b), (c), and (d), respectively. Epidemic parameters are $\beta = 0.1$ and $v = 0.1$. Each point is the average value of 10^2 experiments.

been immunized continuously from epidemic season S to S' ($S < S'$). Plotting $A_{10}(S)$ for $S = 2,3,\ldots,9$ yields the curve in Fig. 7. Here we set $S' = 10$, which is large enough for real cases (the interval between two epidemics may be a year or so in reality). We neglect the epidemic season $S = 1$ because it is a uniform immunization.

However, if we remove the "continuous" condition and concentrate on the total number of times that a node has been vaccinated, we obtain Fig. 8. Here $F_{S'}(i)$ is defined as the ratio of the number of nodes that have been immunized for i times (not necessarily continuously) from the second epidemic

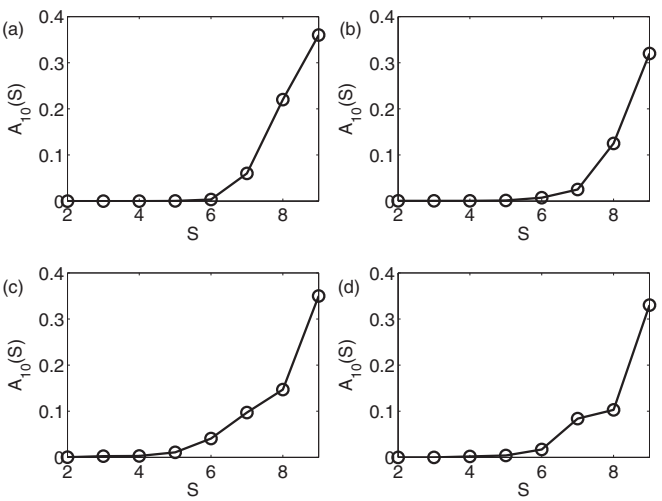

FIG. 7. The relationship between $A_{10}(S)$ and epidemic season S. Results of Wiki-Vote network, Epinions network, Slashdot network, and Enron network are shown in (a), (b), (c), and (d), respectively. Epidemic parameters are $\beta = 0.1$ and $v = 0.1$. Each point is the average value of 10^2 experiments.

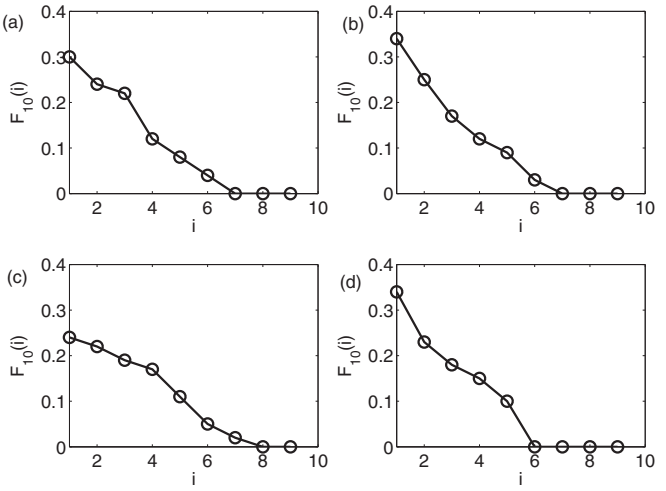

FIG. 8. The relationship between $F_{10}(i)$ and the number of epidemic seasons i. Results of Wiki-Vote network, Epinions network, Slashdot network, and Enron network are shown in (a), (b), (c), and (d), respectively. Epidemic parameters are $\beta = 0.1$ and $v = 0.1$. Each point is the average value of 10^2 experiments.

season to epidemic season S' ($S' > 2$) to the total number of nodes that have been immunized for at least one epidemic season. The first epidemic season is also neglected because of its randomness. Here we also set $S' = 10$. Naturally, we have $F_{10}(1) + F_{10}(2) + \cdots + F_{10}(9) = 1$. In Fig. 8, we can see that more than 10% of the nodes are vaccinated for four epidemic seasons. Combining Figs. 7 and 8, we can see that more than 10% of the nodes are vaccinated for four epidemic

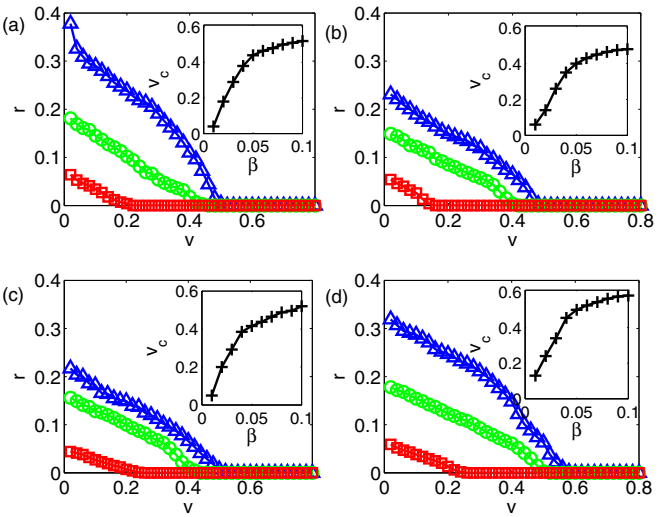

FIG. 9. (Color online) Main plot: The relationship between epidemic prevalence $r_\infty^{(S)}$ and immunization proportion v for different infected rates β. Here $S = 5$. Blue triangles, green circles, and red squares stand for the case of $\beta = 0.10$, 0.05, and 0.02, respectively. Inset: The relationship between vaccinated threshold v_c and β. Here v_c is the value of immunization proportion that makes $r_\infty^{(5)} < 0.005$. Results of Wiki-Vote network, Epinions network, Slashdot network, and Enron network are shown in (a), (b), (c), and (d), respectively. Each point is the average value of 10^2 experiments.

seasons [$F_{10}(4) > 0.1$], but few of them can be vaccinated for more than four continuous epidemic seasons [$A_{10}(6) \approx 0$]. Therefore, we may draw the conclusion that there are some "core individuals" in the evolution. In every epidemic season, the vaccinated nodes are a group of "core individuals" (some global hubs and some local hubs), with the existence of some other nodes. Different "core groups" emerge repeatedly but not continuously.

Now, we concentrate on the critical vaccinated proportion that can halt virus. The v_c obtained in Eq. (5) is actually for uniform immunization and is extremely large (as shown in Table I). Here we fix the infected rate β and vary the immunization proportion v to observe the epidemic prevalence r_∞. As the main plot of Fig. 9 suggests, the curves represent the relationship between r and v, which is almost linear initially and then drops to zero. Obviously, increasing the immunization proportion is an effective method to diminish the epidemic prevalence. In the inset of Fig. 9, we draw the curve of vaccinated threshold v_c that varies by the infected rate β. This provides an estimation of the immunization proportion that inhibits epidemics totally. Obviously, the vaccinated threshold of our method decreases dramatically compared with the uniform cases.

In addition, as for the parameters discussed in Figs. 6–9, the results of the BA network show a similar trend to those four networks.

V. CONCLUSION AND OUTLOOK

To summarize, we have proposed a model to describe seasonal epidemics, and we have presented a related immunization strategy. The selection of vaccinated nodes is optimized gradually, based on the local information of the network from the previous epidemic season. We establish the theoretical framework of our model, which is in agreement with the simulation. We also compare our method with other immunization strategies and find that our method performs better than uniform immunization and acquaintance immunization. These findings suggest that our method provides useful hints for immune strategy design. Meanwhile, we discuss the evolution of vaccinated individuals, and we find that the influential nodes are vaccinated repeatedly but not continuously. As epidemic season continues, the selection of vaccinated nodes tends to remain stable, and they are located in both global and local hubs. We also present the numerical relationship between epidemic prevalence and immunization proportion.

In future research, we would like to discuss the relationship between epidemic prevalence and network structure with our strategy, especially for community structure and correlated networks [4]. In addition, the property of "core individuals" is also an interesting topic that can be studied in more depth.

ACKNOWLEDGMENTS

This work is supported by Major Program of National Natural Science Foundation of China (No. 11290141), NSFC (No. 11201018), International Cooperation Project No. 2010DFR00700, Fundamental Research of Civil Aircraft No. MJ-F-2012-04, and Beihang University Innovation And Practice Fund For Graduates.

[1] D. J. Watts and S. H. Strogatz, Nature (London) **393**, 440 (1998).
[2] R. Pastor-Satorras and A. Vespignani, Phys. Rev. Lett. **86**, 3200 (2001).
[3] M. E. J. Newman, Phys. Rev. E **66**, 016128 (2002).
[4] M. E. J. Newman, SIAM Rev. **45**, 167 (2003).
[5] S. Yan, S. Tang, S. Pei, S. Jiang, X. Zhang, W. Ding, and Z. Zheng, Physica A **392**, 3846 (2013).
[6] A. Barrat, M. Barthelemy, and A. Vespignani, *Dynamical Processes on Complex Networks* (Cambridge University Press, Cambridge, 2008).
[7] W. Li, S. Tang, S. Pei, S. Yan, S. Jiang, X. Teng, and Z. Zheng, Physica A **397**, 121 (2013).
[8] S. Pei and H. A. Makse, J. Stat. Mech. (2013) P12002.
[9] R. Pastor-Satorras and A. Vespignani, Phys. Rev. E **65**, 036104 (2002).
[10] Z. Dezsó and A. L. Barabási, Phys. Rev. E **65**, 055103 (2002).
[11] R. Cohen, S. Havlin, and D. ben-Avraham, Phys. Rev. Lett. **91**, 247901 (2003).
[12] Z. Liu, Y. C. Lai, and N. Ye, Phys. Rev. E **67**, 031911 (2003).
[13] B. Dybiec, A. Kleczkowski, and C. A. Gilligan, Phys. Rev. E **70**, 066145 (2004).
[14] N. Madar, T. Kalisky, R. Cohen, D. ben-Avraham, and S. Havlin, Eur. Phys. J. B **38**, 269 (2004).
[15] J. Gómez-Gardeñes, P. Echenique, and Y. Moreno, Eur. Phys. J. B **49**, 259 (2006).
[16] J. C. Miller and J. M. Hyman, Physica A **386**, 780 (2007).
[17] Y. Chen, G. Paul, S. Havlin, F. Liljeros, and H. E. Stanley, Phys. Rev. Lett. **101**, 058701 (2008).
[18] L. B. Shaw and I. B. Schwartz, Phys. Rev. E **81**, 046120 (2010).
[19] C. M. Schneider, A. A. Moreira, J. S. Andrade, S. Harvlin, and H. J. Herrmann, Proc. Natl. Acad. Sci. USA **108**, 3838 (2011).
[20] J. Ginsberg, M. H. Mohebbi, R. S. Patel, L. Brammer, M. S. Smolinski, and L. Brilliant, Nature (London) **457**, 1012 (2009).
[21] E. Augeraud-Véron and N. Sari, J. Math. Biol. **68**, 701 (2014).
[22] H. W. Hethcote, SIAM Rev. **42**, 599 (2000).
[23] J. C. Frauenthal, *Mathematical Modelling in Epidemiology* (Springer-Verlag, Berlin, 1980).
[24] R. M. Anderson and R. M. May, *Infectious Diseases in Humans* (Oxford University Press, Oxford, 1992).
[25] P. Holme and M. E. J. Newman, Phys. Rev. E **74**, 056108 (2006).
[26] R. M. May and A. L. Lloyd, Phys. Rev. E **64**, 066112 (2001).
[27] M. E. J. Newman, Phys. Rev. Lett. **89**, 208701 (2002).
[28] A. Barrat, M. Barthélemy, and A. Vespignani, *Dynamical Processes on Complex Networks* (Cambridge University Press, Cambridge, 2008).
[29] R. Albert and A. L. Barabási, Science **286**, 509 (1999).
[30] S. N. Dorogovtsev, A. V. Goltsev, and J. F. F. Mendes, Phys. Rev. Lett. **96**, 040601 (2006).
[31] M. Kitsak, L. K. Gallos, S. Havlin, F. Liljeros, L. Muchnik, H. E. Stanley, and H. A. Makse, Nat. Phys. **6**, 888 (2010).

[32] S. Pei, L. Muchnik, J. S. Andrade, Jr., Z. Zheng, and H. A. Makse, Sci. Rep. **4**, 5547 (2014).
[33] http://snap.stanford.edu
[34] L. Backstrom, D. Huttenlocher, J. Kleinberg, and X. Lan, in *Proceedings of the 12th ACM SIGKDD International Conference on Knowledge Discovery and Data Mining* (ACM, New York, 2006), pp. 44–54.
[35] L. Muchnik, S. Pei, L. C. Parra, S. D. S. Reis, J. S. Andrade, Jr., S. Havlin, and H. A. Makse, Sci. Rep. **3**, 1783 (2013).
[36] D. Liben-Nowell and J. Kleinberg, Proc. Natl. Acad. Sci. USA **105**, 4633 (2008).
[37] M. Boguná, R. Pastor-Satorras, and A. Vespignani, Phys. Rev. Lett. **90**, 028701 (2003).